



INFLUENCE OF FLEXURAL CRACKING ON STIFFNESS OF CONCRETE DIAPHRAGMS SUPPORTING HIGH-RISE SHEAR WALLS

Maryam Mahmoodi

PhD Candidate, University of British Columbia, Canada
mmahmoodi@civil.ubc.ca

Perry Adebar

Professor and Department Head, University of British Columbia, Canada
adebar@civil.ubc.ca

ABSTRACT: Concrete shear walls are often supported at the top of a podium structure or at grade by stiff floor diaphragms connected to perimeter walls such as foundation walls. When a large portion of the overturning moment in the tower walls is transferred to the perimeter walls by force couples in two or more stiff floor diaphragms, the maximum bending moment in the tower walls occurs above the upper supporting diaphragm and the shear force reverses below that diaphragm. The magnitude of the reverse shear force, which may be several times larger than the base shear force, depends on the stiffness of the floor diaphragms. As these large shear forces are of considerable concern, it is very important to be able to make an accurate estimate of the diaphragm stiffness. A numerical investigation was conducted to examine the influence of flexural cracking on stiffness of diaphragms supporting high-rise concrete shear walls. A parametric study was carried out to investigate the effects of parameters including the diaphragm length-to-depth ratio, the diaphragm reinforcement ratio and the magnitude of loading. A trilinear force - deformation model was proposed for the stiffness and strength of uncracked diaphragms. To account for the effect of cracking on the initial stiffness of diaphragms in a simple yet accurate way, a simplified equation was developed for cracked diaphragms. To validate the proposed models, the results of the analysis were compared with predictions from the models.

1. Introduction

Concrete shear walls are popular seismic force resisting systems for high-rise buildings as they provide good lateral drift control during earthquakes and are simple to construct. A typical concrete high-rise building has core shear walls located near the centre of the building plan. The core typically extends from the top of the tower down to the foundation. Often the core is supported near the base by a structure that is entirely or partially below ground. The large underground structure is surrounded by rigid perimeter foundation walls. The lateral seismic forces in high-rise walls are transferred to the perimeter foundation walls by interconnecting floor diaphragms below the base. The multiple levels of floor diaphragms also transfer the over-turning moments from the high-rise walls to the perimeter foundation walls. The reduction in bending moment in the high-rise walls is accompanied by a corresponding reverse shear force in the wall section below ground.

The diaphragm action of concrete floor slabs provides an interaction between the core wall and the foundation walls. When a large portion of the overturning moment in the core wall is transferred to the foundation walls by force couples in two or more stiff floor diaphragms, the maximum bending moment (flexural plastic hinge) occurs above the diaphragms and the shear force reverses below the base level. This is known as 'reverse shear force' or 'backstay effect'. One of the important parameters that significantly affects the magnitude of the reverse shear force is the stiffness of floor diaphragms. The larger the diaphragm stiffness, the larger the shear reverse force (Bevan-Pritchard et al. 1983; and Rad and Adebar, 2009).

There are different parameters that influence the stiffness of reinforced concrete floor diaphragms. One of these parameters is the presence of flexural cracks (Chen, 1986). According to the literature, this parameter is not typically taken into account. Indeed, out-of-plane bending moments due to the gravity loads can induce flexural cracking along the reinforced concrete diaphragms which would consequently reduce the initial in-plane stiffness of the diaphragm. This study was conducted to numerically quantify the influence of flexural cracking on the stiffness of concrete floor diaphragms. Based on the numerical results, an approximated trilinear model was developed for force-deformation relationship of uncracked diaphragms. In addition, a simplified equation and procedure was proposed to evaluate the stiffness of cracked diaphragms.

2. Numerical Study

The numerical investigation includes the evaluation of the effect of different parameters on the stiffness of concrete diaphragms. These parameters include the diaphragm length-to-depth ratio, diaphragm reinforcement ratio and loading conditions. In this research work, one span of a continuous concrete slab with a unit width was considered for analysis. The thickness of all analyzed slabs was 200 mm (approx. 8 in.). The slab lengths were assumed to be 4 m (short span) and 7 m (long span) representing the slab length-to-depth ratios of 20 and 35, respectively. The slab was analyzed under two different vertical loading conditions. The first loading case (case 1) accounts for the effect of dead load only (self weight of slab, 4.8 kPa, plus the superimposed dead load, 1.5 kPa) and the second loading case (case 2) accounts for both the dead load and the live load (6.3 kPa + 2.4 kPa). After applying the service gravity loads, the slab was subjected to an increasing tensile force. For simplicity, the translational and rotational displacements were assumed to be restrained on both ends of the slab except for the horizontal displacement at one end which was free to translate.

Two different reinforcement ratios (A_s/A_g) representing lightly reinforced and heavily reinforced slabs were selected. For the slab with light reinforcement, the ratio of the top and bottom reinforcement were 0.5% and 0.25%, respectively. For the slab with heavy reinforcement, the ratio of the top and bottom reinforcement was 1% and 0.75%, respectively. The slab cross section was not symmetric in terms of the amount of reinforcement at the top and bottom of the section.

The 7m slab with light and heavy reinforcement under loading case 1 was designated LR-C1-7 and HR-C1-7, in which "LR" and "HR" stand for light reinforcement and heavy reinforcement, respectively. "Cn" indicates the loading case and the last number is the slab length. Similar designations were used for other analyzed members. A total number of eight slabs were analyzed. Table 1 lists the characteristics of each analysis.

Table 1 - Characteristics of the analyzed slabs

Slab	Reinforcement Ratio	Loading (kPa)	Slab Length (m)
	(A_s/A_g) Top / Bottom		
LR-C1-4	0.005 / 0.0025	6.3	4
LR-C2-4	0.005 / 0.0025	8.7	4
HR-C1-4	0.01 / 0.0075	6.3	4
HR-C2-4	0.01 / 0.0075	8.7	4
LR-C1-7	0.005 / 0.0025	6.3	7
LR-C2-7	0.005 / 0.0025	8.7	7
HR-C1-7	0.01 / 0.0075	6.3	7
HR-C2-7	0.01 / 0.0075	8.7	7

Since the slab is symmetric with respect to its centre-line, half of the slab was considered for the analysis. In order to analyze the slab under the effect of tension and out-of-plane bending moment simultaneously, half of the slab length was evenly divided into twenty segments. For each loading case, the magnitude of the service moment was determined at twenty one sections along the slab span including both ends.

Computer program Response2000 was used to perform the sectional analysis for each section subjected to the calculated bending moment and increasing tensile load with an increment step of 1 kN. The tensile force was increased until the failure of the section reached. The axial load and the corresponding strain at mid-height of the slab was plotted for the twenty one analyzed sections along the slab. Fig. 1 depicts the variation of the strain along the half of the span for the 7 m slab with light reinforcement under loading case 2 (LR-C2-7) and larger strains were observed at supports and the slab mid-span due to the flexural cracking which caused by the presence of gravity loads. The strain linear interpolation was used to evaluate the strain values for each specified axial load at all sections along the slab. By taking the average of these strains, the amount of strain along the slab for the specified axial load was evaluated.

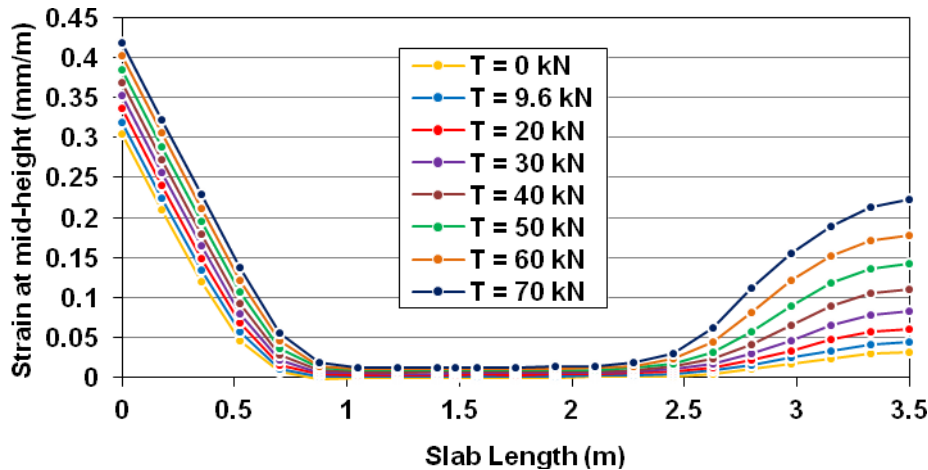


Fig. 1 - Variation of strain at mid-height along half the span for slab LR-C1-7 (0.005 / 0.0025; 6.3 kPa; 7m)

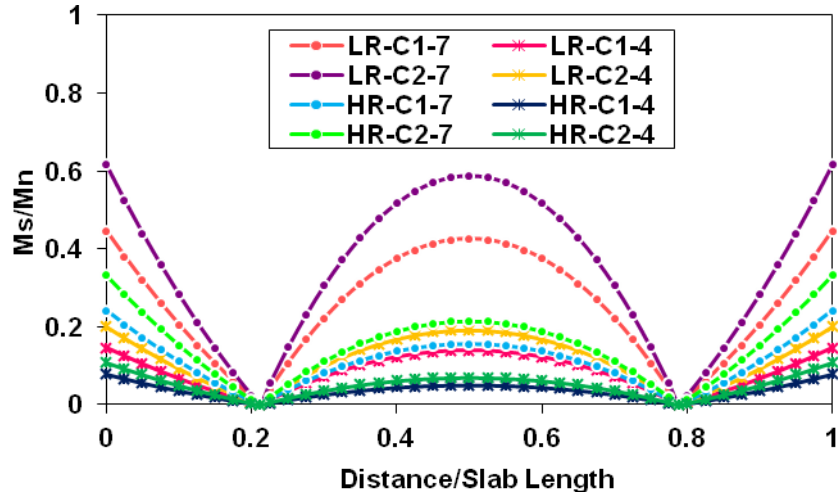
Fig. 2(a) and (b) compare the ratios of the service bending moment (M_s) to the capacity moment (M_n) and the cracking moment (M_{cr}) of the slab for the eight analyzed slabs. The horizontal axis was normalized based on the slab length. The capacity moment of the slab is calculated based on the thickness of the slab and the amount of longitudinal reinforcement. Due to the unsymmetrical top and bottom reinforcement of the slab, the capacity moments of slab at the mid-span and the supports would not be similar. The service moment depends on the applied service gravity loads on the slab as well as the slab length. Therefore, the ratio of the service to the capacity moment is different for the eight analyzed members as shown in Fig. 2(a). The 7 m slab with light reinforcement and loading case 2 had the highest ratio of the service moment to the capacity moment.

The cracking moment is computed based on the thickness of the slab and the concrete tensile strength. Since the slab thickness and concrete tensile strength remained unchanged, the cracking moment was the same for all slabs. Therefore, the slabs with the same length and loading case have the same ratio of the service to the cracking moment (e.g., LR-C1-7 and HR-C1-7 have the same service to cracking moment ratio). According to Fig. 2(b), the flexural cracking due to the presence of gravity loads occurred in the 7 m slabs at the mid-span and both supports while the 4 m slabs did not crack.

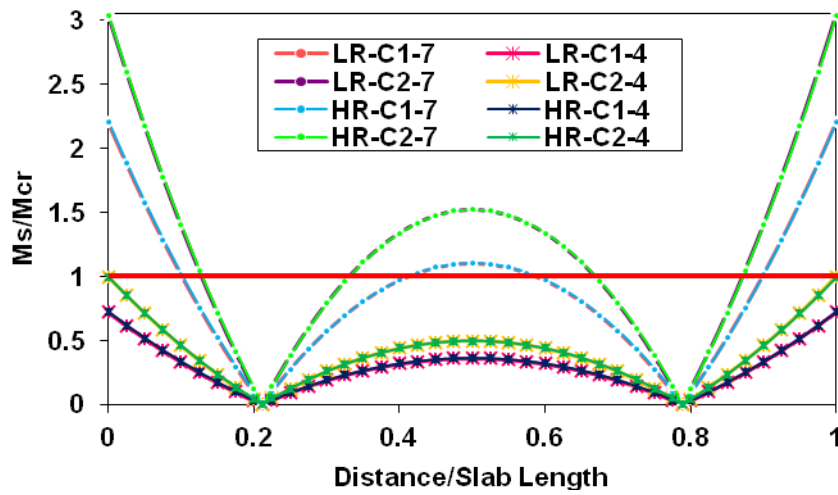
3. Results and Discussion

3.1. Force - Deformation Behaviour

The tensile force versus average strain curves for 4 m slabs with light reinforcement and two loading cases are shown in Fig. 3. The results were compared to the curve obtained from the analysis of the slab subjected to tensile force only. It was observed that when the slab is subjected to tensile force only, there is a high cracking force which is reduced considerably after cracking of the slab. By increasing the tensile force, the stiffness of the slab decreases until the reinforcement is reached the yield level. Due to the asymmetry of the top and bottom reinforcement, the bottom reinforcement yields first and causes strain gradient through the section. A bending moment is developed due to the strain gradient which results in a compression force in the section. Therefore, the tensile strength reduces and the top reinforcement yields.



a)



b)

Fig. 2 - Ratio of service moment to: (a) moment capacity; and (b) cracking moment of slabs

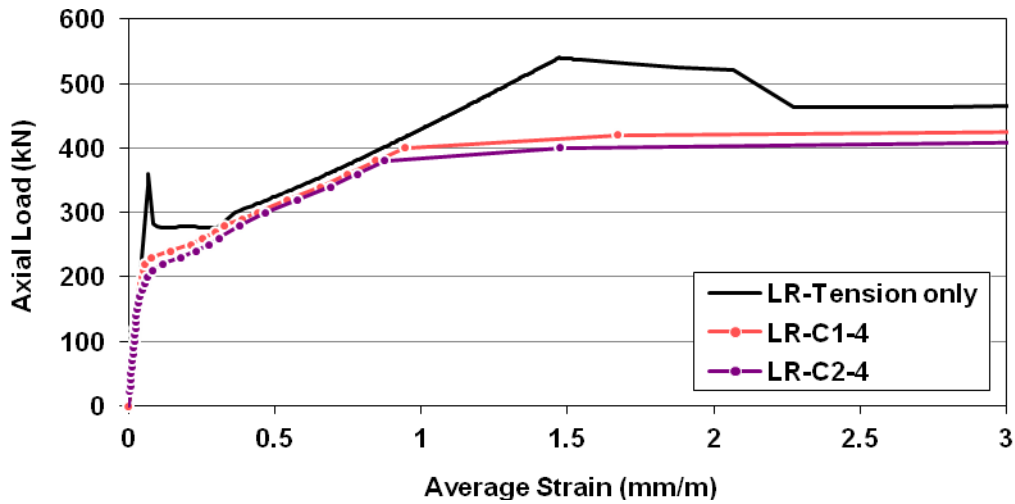


Fig. 3 - Axial load versus average strain for 4 m slabs with light reinforcement

The obtained results showed that the initial stiffness of the 4 m slabs was exactly the same as that of the slab under tensile force only. Therefore, for 4 m slabs, no stiffness reduction was observed but the cracking force of the slab was significantly reduced due to the effect of the bending moment. As shown in Fig. 2, flexural cracking did not occur in 4 m slabs due to the applied gravity loads. Therefore, the initial stiffness of the slab did not decrease. However, a small amount of reduction in the strength of the slab was observed.

Figs. 4 and 5 depict the axial load versus average strain curves obtained from the analyses of the 7 m slabs with light and heavy amount of reinforcement, respectively. The results were compared to the ones obtained from the analysis of the slab subjected to tension force only (no gravity loads). The close up detail of the initial stiffness for the two plots are shown in Fig. 6. Comparison of Figs. 4 and 5 points out that the bending moment considerably influences the behaviour of the tensile force - average strain of the diaphragm when the magnitude of the applied tensile force is relatively small. By increasing the tensile force, this effect decreases. Therefore, for high reinforcement ratios, the yield strength of the slab is large and the influence of bending moment is diminished. Thus, the tensile force - average strain curve of the slab would converge to that of the diaphragm subjected to the tensile force only. However, for low reinforcement ratios, the effect of bending moment is more dominant. It was observed that the initial stiffness of the analyzed 7 m concrete floor slabs decreased significantly. This can be explained by the fact that these slabs were cracked at the location of supports and mid-span by gravity loads before the application of the tensile load. Therefore, the cracking of the slab caused by the vertical loads was believed to be responsible for this stiffness reduction. In addition, an appreciable reduction in the tensile strength of the 7 m slabs with light reinforcement was observed.

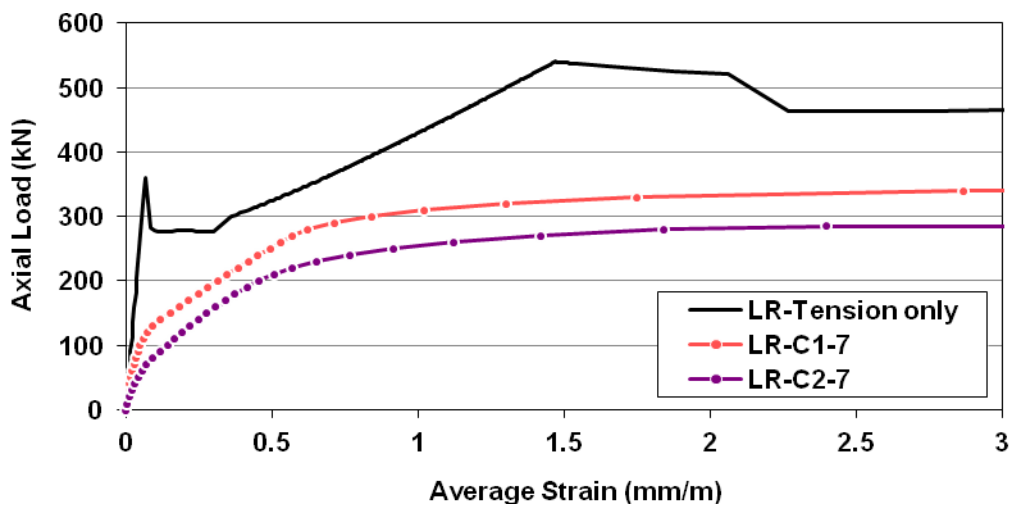


Fig. 4 - Axial load versus average strain for 7 m slabs with light reinforcement

It was observed that the initial stiffness of the analyzed 7 m concrete floor slabs decreased significantly. This can be explained by the fact that these slabs were cracked at the location of supports and mid-span by gravity loads before the application of the tensile load. Therefore, the cracking of the slab caused by the vertical loads was believed to be responsible for this stiffness reduction. In addition, an appreciable reduction in the tensile strength of the 7 m slabs with light reinforcement was observed.

According to Fig. 6, it is obvious that the initial stiffness reduction of the slab LR-C2-7 is larger than that of the other slabs. This can be explained by looking at the strain values along the slabs. Fig. 7 compares the variation of strains at mid-height of the slab along the half of the span for all 7 m slabs when the applied axial load is 100 kN. The strain values are substantially larger for the slab LR-C2-7 along the span. Comparison of the strain values of the slabs LR-C1-7 and LR-C2-7, it was indicated that the difference in the magnitude of the applied service bending moments (different loading cases) caused more cracks along the slab and consequently larger strains in the slab LR-C2-7. In addition, the difference between the strains of the slabs LR-C2-7 and HR-C2-7 can be attributed to the fact that the amount of reinforcement has a direct effect on the yield force as well as the crack control. The larger the reinforcement ratio, the larger the yield force and the smaller the strain values along the slab length.

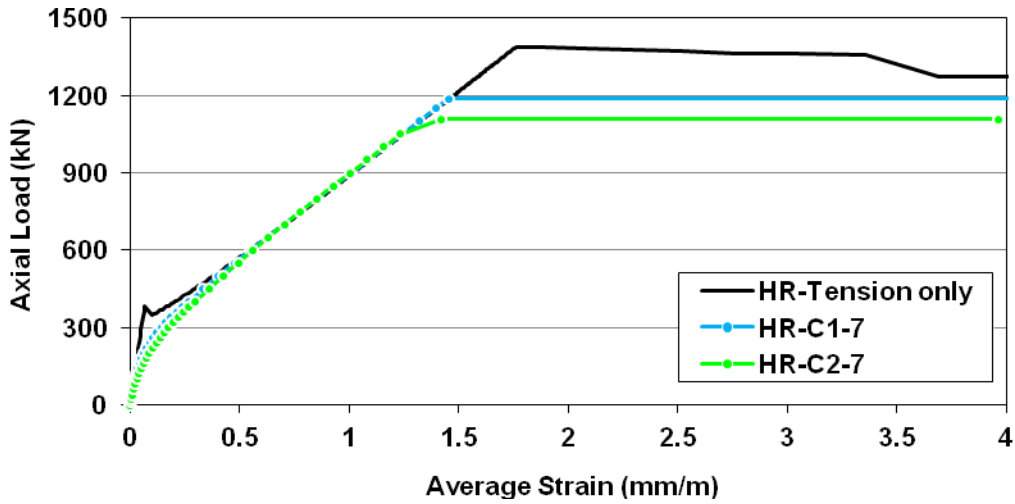


Fig. 5 - Axial load versus average strain for 7 m slabs with heavy reinforcement

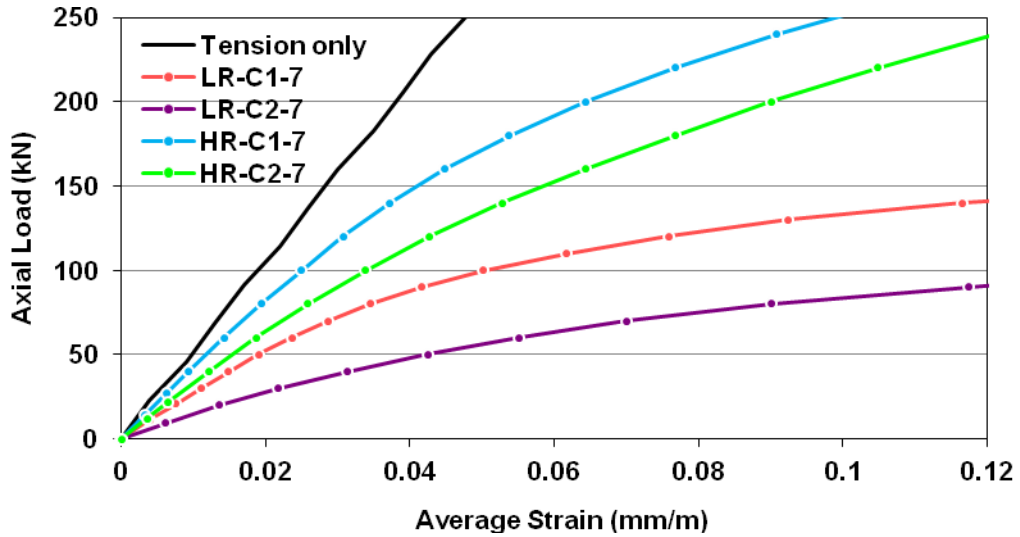


Fig. 6 - Axial load versus average strain for 7 m slabs

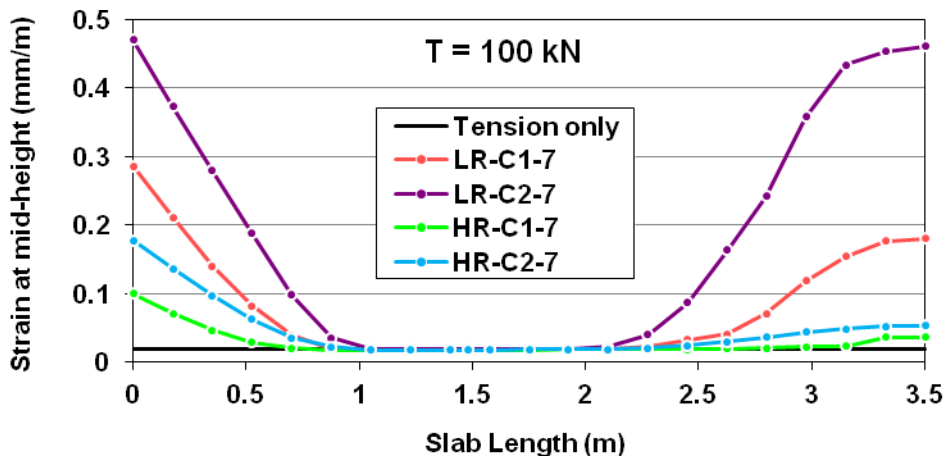


Fig. 7 - Variation of strains along the half of the span for 7 m slabs when axial load is 100 kN

3.2. Diaphragm Tensile Stiffness

Fig. 8 illustrates the ratio of the secant stiffness, K_s , to the tangent stiffness, K_t , versus the average strain at the mid-height of the slab for the initially cracked slab due to the presence of the gravity loads. By comparing the results of the lightly and heavily reinforced slabs under two loading conditions (i.e., Case1 and Case2), it is concluded that the effect of loading conditions (magnitude of bending moments) are more significant at small average strain levels. This effect becomes negligible at higher strain levels as depicted in Fig.8 . In other words, for the slabs with the same reinforcement ratios, the ratio of the secant to the tangent stiffness converges to the same value as the average strain at mid-height of the slab increases.

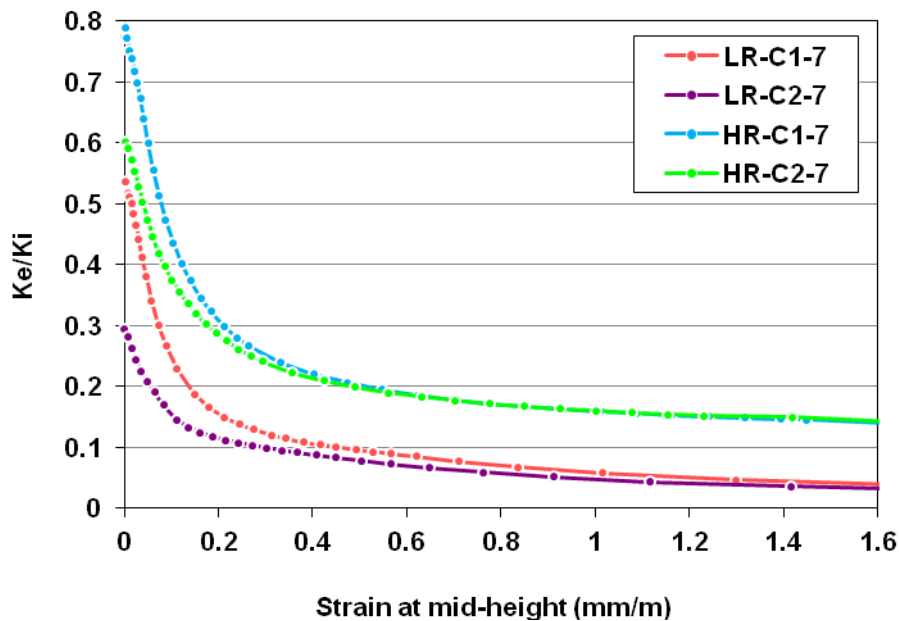


Fig. 8 - Ratio of secant stiffness to tangent stiffness versus average strain for all 7 m slabs

It was observed that when the magnitude of the service moment is less than the cracking moment of the diaphragm ($M_s < M_{cr}$), there would be no reduction in initial stiffness of the diaphragm. In this case, the force-deformation relationship of the diaphragm can be reasonably approximated by a trilinear model. Fig. 9 illustrates the developed trilinear model for force-deformation relationship of uncracked diaphragms. The trilinear relationship is defined by four parameters: (1) the slope of the first straight line segment, $E_c A_g$, (2) the slope of the second straight line segment, (3) the tensile force off-set (shown by "x" in Fig. 9), $f_{cr} A_c / 2$, and (4) the tensile strength of the section under bending and tension, T_y .

The gross section stiffness, $E_c A_g$, is mathematically defined as a product of the concrete modulus of elasticity and the gross sectional area. The second parameter can be determined as a ratio of the tensile strength of the section, T_n , to the yield strain of steel, ϵ_y , which is approximately 0.002 for steel Grade 400. The tensile strength of the section can be obtained by hand calculation which primarily depends on the amount of reinforcement. In fact, this parameter is equal to the product of the modulus of elasticity of steel and the area of reinforcing bars, $E_s A_s$, for a section with symmetric top and bottom reinforcement. However, for the section with unsymmetrical reinforcement, there would be some reduction in the tensile strength of the section due to the strain gradient which should be considered in the calculation. The third parameter is the distance "x" as shown in Fig. 9. This distance is defined as the tensile force difference between the second line segment of the trilinear model and the line representing no tension stiffening effect of concrete (green line in Fig. 9) at a certain level of strain. This parameter is approximated by half of the cracking force of the section, where $f_{cr} = 0.3(f'_c)^{1/2}$ is the cracking strength of concrete. The final parameter that is required to define the trilinear force-deformation relationship of uncracked diaphragms is the tensile strength under bending moment and tension force simultaneously, T_y , which corresponds to the force that both top and bottom reinforcements yield. In order to define this parameter, the tensile strength

of the slab should be calculated at the most critical sections along the slab which are at the supports and mid-span. The smaller of the obtained values is considered as the tensile strength of the slab.

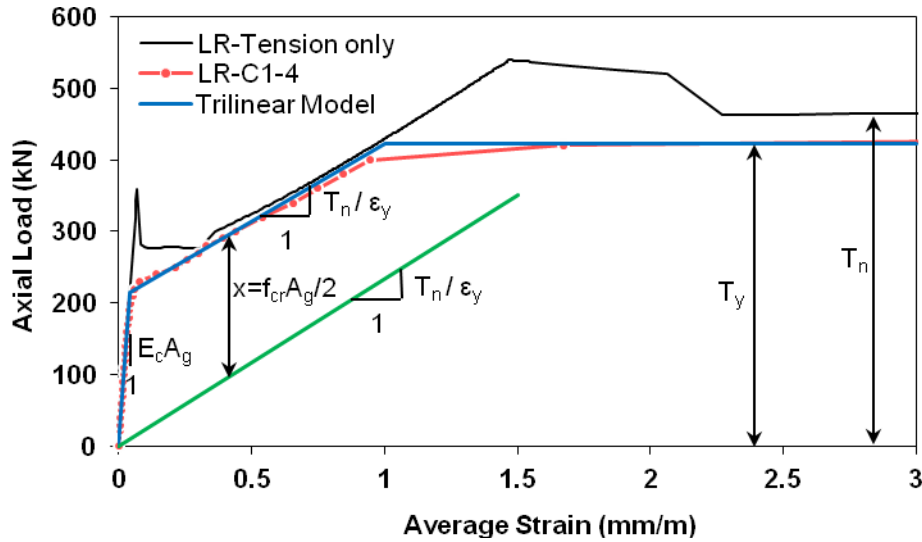


Fig. 9 - Trilinear idealization of the force-deformation relationship for uncracked diaphragms

When the magnitude of the applied service moment is larger than the cracking moment of the diaphragm ($M_s > M_{cr}$), the flexural cracking occurs in the diaphragm. It was indicated that the flexural cracking significantly reduces the initial stiffness of the concrete floor diaphragms. The more cracking in the diaphragm, the more reduction in the initial stiffness of diaphragm. Two main parameters that influence the extent of cracking along the diaphragm length are the magnitude of the applied service loads and the diaphragm reinforcement ratio.

Since displacements involve the integration of strains along the length of a diaphragm, the stiffness is related to average strains. In fact, for the initial stages of the analysis, when the applied tensile force is small, the stiffness can be defined as the ratio of the tensile force to the average strain along the diaphragm. The following simple equation was developed to evaluate the stiffness of cracked diaphragms:

$$\frac{1}{K} = \frac{\alpha_1^2}{2E_s A_s^-} + \frac{\alpha_2^2}{4E_s A_s^+} + \frac{\alpha_3}{E_c A_c} \quad (1)$$

where $\alpha_1 = 0.42(1 - M_{cr}/M_s^-)$ and $\alpha_2 = 0.58\sqrt{1 - M_{cr}/M_s^+}$ are determined as a ratio of the cracked length to the diaphragm length at supports and mid-span, respectively. $\alpha_3 = 1 - (\alpha_1 + \alpha_2)$ is defined as a ratio of the uncracked length to the diaphragm length. E_s and E_c are the modulus of elasticity of steel and concrete, respectively. A_s^- , A_s^+ and A_c are the area of top and bottom reinforcement and the concrete cross section area, respectively.

The first term of the equation is proportional to the average of strain increment along the cracked length of the diaphragm at supports due to the small increase of the tensile force. The second term reflects the contribution of the average strain increment along the cracked length of the diaphragm at mid-span. Finally, the third term is obtained from the elastic strain increment along the uncracked length of the diaphragm due to the tensile force increment.

In order to validate the proposed equation for the reduced stiffness of the cracked diaphragm, the diaphragm stiffness predicted by the proposed simple model are compared to that obtained from the analyses and in Fig. 10. There is a good agreement between the results. However, the predicted stiffnesses are larger than the tangent stiffnesses calculated from the analyses. Therefore, the proposed

simplified model estimates the stiffness of cracked diaphragms conservatively which is more desirable for the purpose of this study. In fact, smaller stiffness values would result in smaller reverse shear force which may lead to underestimating the design of the wall for shear.

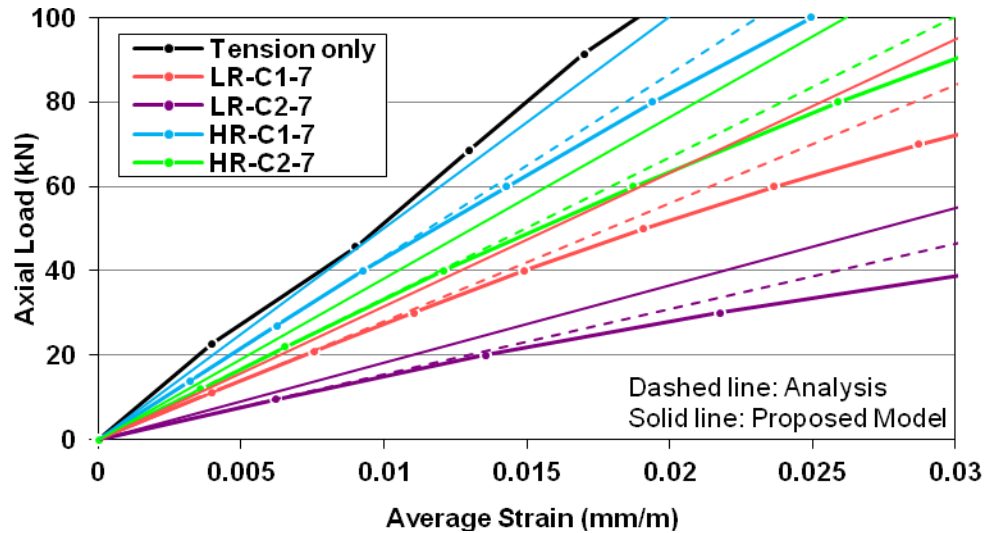


Fig. 10 - Comparison of the stiffness predicted by the proposed model with that obtained from analyses for all 7 m slabs

3.3. Diaphragm Shear Stiffness

In order to evaluate the stiffness of the concrete diaphragm, a simply supported deep beam was considered as shown in Fig. 11. The rigid foundation walls were assumed to perform as lateral supports due to their high lateral stiffness. The core wall's action was modelled by applying two concentrated forces at the location of the shear walls. Only the shear deformation of the diaphragm was taken into account and the flexural deformation was ignored which is relatively small. Therefore, the stiffness of the diaphragm mainly depends on the shear modulus of the diaphragm.

The applied shear forces from core walls are transferred to the perimeter foundation walls through the diaphragms. Thus, the diaphragms behave similar to membrane elements, as shown in Fig. 11. In order to account for the influence of flexural cracking, the reinforced concrete slab can be considered as an orthotropic material with reduced modulus of elasticity due to the influence of the flexural cracking. The effect of cracking was assumed in one direction only which is a more conservative assumption. Cracking of concrete reduces the stiffness of floor diaphragms and the shear reverse force would be accordingly reduced. Based on the literature, the shear modulus of reinforced concrete diaphragms as an orthotropic material can be predicted by Equation 2 which was proposed by Huber (1923) and followed by other researchers in mechanics such as Cheng and He (1984) and Bert (1985):

$$G = \frac{\sqrt{E_1 E_2}}{2(1 + \nu_{12} \nu_{21})} \quad (2)$$

Huber used geometric mean in predicting the shear modulus of reinforced concrete slabs. The modulus of elasticity of concrete in the direction of cracking can be determined based on the present study. After cracking of concrete, the Poisson's ratio was assumed to remain unchanged and equal to 0.25 which is its value for concrete in both orthogonal directions. In fact, prior to cracking, the Poisson's ratios, ν_{12} and ν_{21} are identical and equal to 0.25. After cracking, ν_{12} increases gradually to a higher value of about 1.9 and ν_{21} decreases rapidly to a small value and then gradually approaches zero (Zhu, 2000). When ν_{21} approaches zero, the product of the Poisson's ratios becomes close to zero. Therefore, the denominator of the Equation 2 becomes equal to 2 which is 2.5 for uncracked concrete. This means that the shear

modulus of the cracked concrete becomes larger than that of the uncracked concrete which is not acceptable. Therefore, the assumption of equal Poisson's ratios of 0.25 in both orthogonal directions is more reasonable. After defining the shear modulus of cracked concrete, the diaphragm stiffness can be easily determined based on the diaphragm length-to-width ratio (L/W). In fact, the stiffness of the diaphragm is the shear force per unit deflection of the beam at the location of the applied shear force.

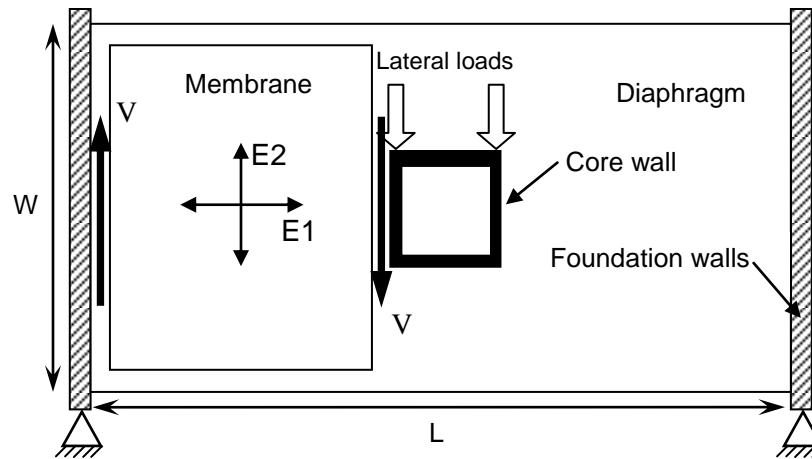


Fig. 11 - Simplified model to define diaphragm stiffness

4. References

- Bentz, E.C., Collins, M.P., "Response 2000." www.ecf.utoronto.ca/~bentz/r2k.htm.
- Bert C. W., "Theory of Orthotropic and Composite Cylindrical Shells, Accurate and Simple Fourth- Order Governing Equations", *Journal of Applied Mechanics*, 52, 1985, 982.
- Bevan-Pritchard, G. L., Man, E., Anderson, D. L., "Force distribution between core and sub-grade structure of high-rise buildings subjected to lateral load induced forces", *Proc., 4th Canadian Conf. on Earthquake Eng.*, CAEE, Vancouver, 1983, pp. 210-219.
- Chen, S. J., "Reinforced Concrete Floor Slabs under In-Plane Monotonic and Cyclic Loading", Ph.D. thesis, 1986, Department of Civil Engineering, Lehigh University, Bethlehem, Pennsylvania, USA.
- Cheng, S., He, F., "Theory of orthotropic and composite cylindrical shells, accurate and simple fourth-order governing equations", *Journal of Applied Mechanics*, 51, 1984, pp. 736-744.
- Humber, M., "The theory of crosswise reinforced ferroconcrete slabs and its application to various important constructional problems involving rectangular slabs", *Der Bauingenieur* 4, 12, 1923. pp. 354-360.
- Rad, R. B., Adebar, P., "Seismic Design of High-Rise Concrete Walls: Reverse Shear due to Diaphragms below Flexural Hinge", *Journal of Structural Engineering (ASCE)*, 2009, pp. 916-924.